Flexural Behavior of Brittle RC Members Rehabilitated with Concrete Jacketing

G.E Thermou[1], S.J. Pantazopoulou[2], M. ASCE and A.S. Elnashai[3], F. ASCE

Abstract: The composite flexural action of prismatic reinforced concrete (RC) members repaired / strengthened by RC jacketing was modeled with a dual-section approach. The model considers the relative slip at the interface between the existing member and the jacket and establishes the mechanisms that are mobilized to resist this action thereby supporting composite behavior. An iterative step-by-step incremental algorithm was developed for calculating the overall flexural response curve. Consideration of frictional interlock and dowel action associated with sliding at the interfaces as well as the spacing and penetration of flexure-shear cracks are key aspects of the algorithm. The proposed procedure was verified through comparison with published experimental data on RC jacketed members. The sensitivity of the upgraded member's flexural response to jacket design variables was investigated parametrically. Monolithic response modification factors related to strength and deformation indices were evaluated and the sensitivity of the model was assessed.

CE Database subject headings: Reinforced concrete; Shear transfer; Rehabilitation; Interface stress; Seismic design.

[1] PhD Candidate, Dept. of Civil Engineering, Laboratory of Reinforced Concrete, Demokritus University of Thrace, Vas. Sofias 12, Xanthi 67100, Greece, email: gthermou@civil.duth.gr

[2] Professor, Dept. of Civil Engineering, Laboratory of Reinforced Concrete, Demokritus University of Thrace, Vas. Sofias 12, Xanthi 67100, Greece, email: pantaz@civil.duth.gr, tel/fax: +30-25410-79639

[3] Bill and Elaine Hall Endowed Professor, Dept. of Civil and Environmental Engineering, University of Illinois at Urbana-Champaign, 2129 Newmark CE Lab., 205 North Mathews Avenue, Urbana, IL, 61801, USA, Tel.: 217-265-5497, Fax: 217-265-8070, E-mail: aelnash@uiuc.edu.

INTRODUCTION

Reinforced concrete jacketing is a traditional method for seismic upgrading of damaged or poorly detailed reinforced concrete construction. In applying this technique, the objective is to suppress alternative premature modes of failure that would otherwise prevail in the structural members under reversed cyclic loading, thereby promoting flexural yielding of primary reinforcement. Through RC jacketing stiffness and strength are increased, whereas dependable deformation quantities may or may not be enhanced, depending on the aspect ratio of the upgraded element and the factors limiting deformation capacity in the initial state of the element. For practical purposes, response indices of the jacketed members such as resistance and deformation measures at yielding and ultimate are routinely obtained by applying pertinent multipliers on the respective properties of monolithic members with identical geometry. The multipliers are referred to in the literature as *monolithic factors*, K_i.

Depending on the member property being scaled (strength or stiffness), the method of load application and the jacket function, various values have been reported for K_i, ranging from 0.7 up to 1. Eurocode 8 (Annex G 1996) recommends K_R=0.8 for strength and K_K=0.7 for stiffness provided that: (1) Loose concrete and buckled reinforcement in the damaged area have been repaired or replaced before jacketing. (2) All new reinforcement is anchored into the beams and slabs. (3) The additional concrete cross section is not larger than twice the cross section of the existing column. Based on the results of a recent experimental study conducted by Vandoros and Dritsos (2006a, 2006b), the monolithic factors associated with strength, stiffness and deformation vary greatly depending on the techniques followed in constructing the jacket. For example, it was shown that dowels improve the ductility capacity of the jacketed member, roughening of the interface increases the energy absorption capacity and a combination of the two procedures improves stiffness.

Monolithic factors are used by Codes of practice for convenience, as the mechanics of composite action of jacketed reinforced concrete members under cyclic shear reversals is too complicated for practical calculations. So far the focus has been on stiffness and strength, whereas no specific reference has been made for monolithic factors related to deformation indices. A detailed method for calculating these factors would be required in order to assess their parametric sensitivity to the relevant design variables. From the available experimental evidence it appears that slip and shear

stress transfer at the interface between the outside jacket layer and the original member that serves as the core of the upgraded element are controlling factors (Eurocode 8 1996; KANEPE 2004). Indeed, sliding failure at the interface limits the strength and affects the rotation capacity of the entire member.

This paper presents a detailed procedure for estimating the behavior of concrete members jacketed with an outer RC shell. The composite action that jacketed reinforced concrete members develop in flexure greatly depends on the force transfer that occurs between the core and the jacket. Estimating strength and deformation capacity of such members is a complex mechanics problem that is hampered by the limited understanding of the interfacial resistance mechanisms such as friction, interlock and dowel action. To calculate the monolithic factors and to establish their dependence on critical design variables an analytical model is developed in this paper from first principles. The significance of jacket detailing on the resulting response and the associated values of the monolithic factors for strength and deformation capacity is demonstrated and quantified through parametric studies and correlation of analytical estimates with test results.

ANALYTICAL MODEL FOR RC JACKETED MEMBERS

It is assumed that the existing member core is partially connected with the external jacket layer, so that the mechanisms of force transfer at the interface are mobilized by relative slip of the two bodies. In analyzing the flexural behavior, the cross section of the upgraded member is divided into three layers. The two external ones represent the contribution of the jacket whereas the middle layer represents both the core (existing cross section) and the web of the jacket shell [Fig. 1(a)]. For reference in the remainder of this derivation, the Cartesian coordinate system is oriented so that the x-axis is parallel to the longitudinal member axis, the y-axis is along the cross-sectional depth, whereas the z-axis is oriented along the cross-sectional breadth [Fig. 1(d)]. The difference in normal strain at the interface between layers accounts for the corresponding slip in the longitudinal direction; thus, only the implications of slip along horizontal planes are considered in the model. The inaccuracy associated with neglecting shear transfer along the vertical contact faces (i.e. on faces normal to the z-axis) is small if jacket longitudinal tension reinforcement is evenly distributed in the perimeter [Fig.

1(a)]. Note that in that case, a vertical slice of the jacketed cross section is self equilibrating (consider for example the rectangular portion of the cross section, to the left of line A-A' in Fig. 1(a)). This means that the total stress resultant is zero since compression and tension forces over the height of the segment are in equilibrium; hence the shear stress τ_{xz} [Fig. 1(d)] acting in a plane normal to the z-axis and oriented in the longitudinal direction is also zero. As usually done in flexural analysis of layered composite beams, it is assumed that the three layers deform by the same curvature, φ [Fig. 1(a)]. From free body equilibrium of any of the two exterior layers the shear flow at the interface is calculated as the difference in the stress resultant between two adjacent cross sections. The procedure is implemented in an iterative algorithm that employs dual-section analysis. A key element of the algorithm is the shear stress slip relationship used to describe the behavior of the interface between layers.

Interface shear behavior

Slip at the interface between the existing member and the jacket is explicitly modeled. Mechanisms that resist sliding are: (1) aggregate interlock between contact surfaces, including any initial adhesion of the jacket concrete on the substrate, (2) friction owing to clamping action normal to the interface, and (3) dowel action of any pertinently anchored reinforcement crossing the sliding plane. Thus, in stress terms, the shear resistance, v_n, against sliding at the contact surface, is:

$$v_n = v_a + v_c + v_D = v_a + \mu\sigma_N + v_D \tag{1}$$

In Eq. (1) v_a represents the shear resistance of the aggregate interlock mechanism, μ is the interface shear friction coefficient, σ_N is the normal clamping stress acting on the interface and v_D is the shear stress resisted by dowel action in cracked reinforced concrete. The first two terms collectively represent the *contribution of concrete* as they depend on the frictional resistance of the interface planes. The clamping stress represents any normal pressure, p, externally applied on the interface, but also the clamping action of reinforcement crossing the contact plane as illustrated in Fig. 1(b). From equilibrium requirements it is shown:

$$\sigma_N = p + \rho_s f_s \tag{2}$$

where p is the normal pressure externally applied on the contact plane, f_s is the axial stress of the bars crossing the interface and ρ_s the corresponding reinforcement area ratio.

Shear transfer is affected by the roughness of the sliding plane, by the characteristics of the reinforcement, by the compliance of concrete and by the state of stress in the interface zone. Dowel action develops by three alternative mechanisms, namely, by direct shear and by kinking and flexure of the bars crossing the contact plane. A variety of models are available for modeling the interface phenomena. In this study, the model developed by Tassios and Vintzēleou (1987) and Vintzēleou and Tassios (1986; 1987) as modified by Vassilopoulou and Tassios (2003) was used due to its simplicity and robustness. The model estimates the combined dowel and shear friction resistances for a given slip value at the interface, as follows:

(a) Frictional Resistance

The concrete contribution term in Eq. (1), $v_c(s)$, is described by the following set of equations:

$$\frac{v_c(s)}{v_{c,u}} = 1.14\left(\frac{s}{s_{c,u}}\right)^{1/3} \quad \text{for} \quad \frac{s}{s_{c,u}} \le 0.5 \tag{3.a}$$

$$\frac{v_c(s)}{v_{c,u}} = 0.81 + 0.19\left(\frac{s}{s_{c,u}}\right) \quad \text{for} \quad \frac{s}{s_{c,u}} > 0.5 \tag{3.b}$$

where $s_{c,u}$ is the ultimate slip value beyond which the frictional mechanisms break down ($s_{c,u}$ is taken approximately equal to 2 mm, CEB-FIP Model Code 90 1993). The normalizing term, $v_{c,u}$, is the ultimate frictional resistance of the interface, given by,

$$v_{c,u} = \mu\left(f_c'^{2}\sigma_N\right)^{1/3} \tag{4}$$

where μ the ultimate interface shear friction coefficient taken equal to 0.4 and f_c' the concrete cylinder uniaxial compressive strength [Fig. 1(b)]. To calculate the axial stress of the bars crossing the interface, f_s, the separation w between contact surfaces as they slide overriding one another is considered [Fig. 1(c)]. According to Tassios and Vintzēleou (1987) the separation w and lateral slip, s, are related by: $w=0.6 \cdot s^{2/3}$. To account for w, it is assumed that the bars pullout by $w/2$ from each side of the contact surface. Considering uniform bond stresses along the embedment length, the axial bar stress, f_s, at the contact plane is estimated from:

$$f_s = \left(\frac{0.3 s^{2/3} E_s f_c^{/}}{D_b} \right)^{1/2} \quad (5)$$

In Eq. (5), E_s is the elastic modulus of steel and D_b is the diameter of the bars clamping the interface (here, the stirrup legs of the jacket).

(b) Dowel Resistance

In the dowel model the bar behaves as a horizontally loaded free-headed pile embedded in cohesive soil. Yielding of the dowel and crushing of concrete are assumed to occur simultaneously. Dowel force [the resultant of term v_D in Eq. (1)] is obtained from the relative interface slip s as follows [Fig. 1(c)]:

$$\frac{V_D(s)}{V_{D,u}} = 0.5 \frac{s}{s_{d,el}} \text{ for } s \le s_{d,el} = 0.006 D_b \quad (6.a)$$

$$\text{for } \frac{V_D(s)}{V_{D,u}} \ge 0.5 \Rightarrow s = 0.006 D_b + 1.76 s_{d,u} \left[\left(\frac{V_D(s)}{V_{D,u}} \right)^4 - 0.5 \left(\frac{V_D(s)}{V_{D,u}} \right)^3 \right] \quad (6.b)$$

where $s_{d,el}$ is the elastic slip value, $s_{d,u}$ is the ultimate slip value, $V_{D,u}$ is the ultimate dowel force and D_b is the diameter of the bars offering dowel resistance (here, legs of the jacket transverse reinforcement).

In Eq. (6.b) the dowel force, $V_D(s)$, is estimated iteratively given the slip magnitude, s. The ultimate dowel strength and associated interface slip are given by:

$$V_{D,u} = 1.3 D_b^2 \left(f_c^{/} f_{sy} (1-\alpha)^2 \right)^{1/2}; \quad s_{d,u} = 0.05 D_b \quad (7)$$

where α is the bar axial stress normalized with respect to its yield value and f_{sy} is the yield strength of steel.

The total shear resistance of an interface with contact area A_{int} crossed by k dowels is:

$$V(s) = v_c(s) A_{int} + k V_D(s) \quad (8)$$

where $v_c(s)$ and $V_D(s)$ are calculated from Eqs. (3) and (6), respectively, for a given amount of interface slip.

Estimation of crack spacing

Similar to conventional bond analysis, shear transfer at the interface between the existing member and

the jacket is carried out between half crack intervals along the length of the jacketed member [Fig. 2(a)]. To evaluate the crack spacing the stress state at the crack is compared with that at the mid-span between adjacent cracks [Fig. 2(b)]. It is assumed that at the initial stages of loading cracks form only at the external layers (jacket) increasing in number with increasing load, up to crack stabilization. This occurs when the jacket steel stress at the crack, $f_{s,cr}$ exceeds the limit (CEB-FIP Model Code 90 1993):

$$f_{s,cr} > f_{ctm} \frac{1+\eta\rho_{s,eff}}{\rho_{s,eff}} \tag{9}$$

where f_{ctm} is the tensile strength of concrete, $\eta(=E_s/E_{cm})$ is the modular ratio and $\rho_{s,eff}$ is the effective reinforcement ratio defined as the total steel area divided by the area of mobilized concrete in tension, usually taken as a circular domain with a radius of $2.5D_b$ around the bar (CEB-FIP Model Code 90 1993). Using the same considerations in the combined section it may be shown that a number of the external cracks penetrate the second layer (core) of the jacketed member [Fig. 2(a)]. From the free body diagram shown in Fig. 2(b) the shear flow, q_s, at the contact between the bottom layer and the core is estimated as:

$$q_s = \pi \frac{N_J D_{b,J}}{b_J} f_{b,J} \tag{10}$$

where N_J is the number of bars in the tension steel layer of the jacket, $D_{b,J}$ is the bar diameter of the jacket longitudinal reinforcement, $f_{b,J}$ is the average bond stress of the jacket reinforcement layer and b_J the width of the jacketed cross section. The crack spacing is estimated from free body equilibrium in the tension zone of the core of the composite section [Fig. 2(b)]. Assuming that the neutral axis depth is about constant in adjacent cross sections after stabilization of cracking, the crack spacing is defined as follows:

$$c = \frac{2\, b_J\, l_c\, f_{ctm,c}}{\pi\, N_c\, D_{b,c}\, f_{b,c} + q_s\, b_J} \tag{11}$$

where N_c is the number of bars in the tension steel layer of the core, $D_{b,c}$ is the bar diameter of the core longitudinal reinforcement, $f_{b,c}$ is the average bond stress of the core reinforcement layer, l_c is the height of the tension zone in the core component of the composite cross section and $f_{ctm,c}$ the tensile strength of concrete core.

Shear stress distribution on the cross section of the jacketed member

To analyze jacketed members in flexure the composite cross section is assumed to deform in its plane of symmetry with a curvature φ; relative slip occurs in the horizontal contact planes between the top and bottom jacket layers and the core [Fig. 1(a)]. Section equilibrium is established and the normal stress resultant of each layer, $\Sigma F_{i,}$ is estimated [Fig. 2(c)]. Using dual-section analysis (Vecchio and Collins 1988), and considering that the shear force at any section equals the moment gradient along the member length, the layer stress resultant ΣF_i, is used to calculate the vertical shear stress demand of the member (i.e., stress τ_{xy}, oriented in the y-axis in Fig. 1(d)), at layer ith, denoted here by term $v_{d,i}$, from:

$$v_{d,i} = \frac{\Sigma F_i}{0.5\, c\, b_J} \tag{12}$$

where c is obtained from Eq. (11) [Fig. 2(a)]. From basic mechanics the vertical shear stress, $v_{d,i}$, is taken equal to the horizontal shear stress ($\tau_{xy} = \tau_{yx}$) mobilized along the interface for a given slip magnitude, s_i.

Deformation estimates at yield and ultimate

The cross section is considered to have attained a state of flexural yielding when the extreme layer of tensile reinforcement reaches first its yield strain (ε_{sy}) or alternatively when the concrete strain at the extreme compression fiber exceeds the limit value of $\varepsilon_c = 1.5‰$ (*fib* Bulletin 24 2003, Chapter 4). Definition of an ultimate state is also adopted so as to allow comparisons between the monolithic and the detailed analytical approach. To this purpose an *equivalent monolithic curvature,* $\varphi_{u,M}^{eq}$, is estimated from the analysis corresponding to a specified target drift at ultimate. The total inelastic displacement comprises the elastic displacement at yield Δ_y, the plastic displacement $\Delta_{p,u}$, and the displacement owing to interface slip $\Delta_{slip,u}$:

$$\Delta_o = \Delta_y + \Delta_{p,u} + \Delta_{slip,u} \tag{13.a}$$

where,

$$\Delta_y = \frac{1}{3}\varphi_y L_s^{\,2};\ \Delta_{p,u} = (\varphi_u - \varphi_y) l_p (L_s - 0.5 l_p);\ \Delta_{slip,u} = \theta_{slip,u} L_s = (s_{1,u} + s_{2,u}) \frac{L_s}{j_d} \quad (13.b)$$

In Eq. (13.b), φ_y is the curvature at yield of the composite section, l_p is the length of the plastic hinge region (taken here as $0.08L_s+0.022D_b f_{sy}$ according to Paulay and Priestley 1992), and φ_u is the curvature at ultimate. Terms in Eq. (13) are calculated using the proposed model and represent the tip displacements of a cantilever having a length L_s equal to the shear span of the member (in seismic loading the cantilever considered represents approximately half the member length under lateral sway). $\Delta_{slip,u}$ is calculated at the ultimate from the slip values at the upper and bottom interfaces, s_{1u} and s_{2u}, as shown in Fig. 2(d). Owing to interface slip the cross section rotates by $\theta_{slip,u}=(s_{1,u}+s_{2,u})/j_d$, where j_d represents the distance between the upper and the bottom interfaces (i.e. j_d equals the core height which is usually the cross sectional height of the old member). Clearly, the end (slip) rotation $\theta_{slip,u}$ is greater for smoother interfaces, and therefore deformation indices of jacketed members are expected to be higher for lower interface friction properties.

The equivalent monolithic curvature, $\varphi_{u,M}^{eq}$, is obtained by assuming equal displacements at ultimate for both the monolithic and the composite members. Therefore,

$$\varphi_{u,M}^{eq} = \frac{\left[\Delta_o - \frac{1}{3}\varphi_{y,M} L_s^2 + \varphi_{y,M} l_p \left(L_s - 0.5 l_p\right)\right]}{l_p (L_s - 0.5 l_p)} \quad (14)$$

In Eq. (14), Δ_o is the total tip displacement [calculated from Eq. (13.a)] and $\varphi_{y,M}$ the curvature at yield of the monolithic cross section obtained from conventional sectional analysis.

CALCULATION ALGORITHM

In the proposed model the interfaces between old concrete and the jacket are treated as the weak link of the composite behavior; thus, the shear force demand introduced in the contact surfaces for any level of flexural curvature cannot exceed the associated interface strength that corresponds to the level of slip already attained. Calculations are performed for monotonically increasing curvature using stepwise iteration. Initially, interface slip is taken to be zero at both contact surfaces. Hence, in the first step of the solution (for very small strains) the longitudinal strain profile is identical to that of the

monolithic approach [Fig. 1(a)]. The shear flow is calculated from dual-section analysis, using the estimated flexural stresses. Based on classical mechanics a longitudinal shear flow (i.e. shear stress τ_{xy} in Fig. 1(d)) may be calculated at any distance y_i [Fig. 1(a)] from the neutral axis of a monolithic elastic cross section, as:

$$q_o = V\, S_i / I \tag{15}$$

where S_i is the first moment of area from y_i to the top of the cross section, I is the moment of inertia of the composite cross section, and V is the shear force on the member calculated from the estimated flexural moment of the monolithic section divided by the shear span, L_s. In the subsequent steps the longitudinal strain gradient is modified (by allowing for sequentially increasing discontinuities of strain at the interface levels) as required to satisfy equilibrium. The interface slip is related to the magnitude of strain discontinuity at the upper and bottom interfaces, $\Delta\varepsilon_1$ and $\Delta\varepsilon_2$, as follows:

$$s_1 = \Delta\varepsilon_1\, c = (\varepsilon_{c1} - \varepsilon_{j2})\, c\,, \quad s_2 = \Delta\varepsilon_2\, c = (\varepsilon_{j3} - \varepsilon_{c2})\, c \tag{16}$$

where variables ε_{c1}, ε_{j2} and ε_{j3}, and ε_{c2} are normal strains in the section layers above and below the contact surfaces [Fig. 1(a)], and c the average crack spacing [Fig. 2(a)]. Interface shear resistance is mobilized depending on the slip magnitude: interface shear resistances v_1 and v_2 [Eq. (1)] are obtained from the respective slip values (s_1 and s_2) using the constitutive relationships for interface behavior [Eqs. (3-8), illustrated in Fig. 2(c)]. Shear demand values ($v_{d,1}$ and $v_{d,2}$), estimated from Eq. (12), are compared with the dependable resistance values [from Eq. (1)] for equilibrium. If equilibrium is not attained then the slip estimate is subsequently revised and the above calculation repeated until convergence. The final step in the algorithm involves establishing equilibrium of forces over the composite member cross section. The strain profile of the cross section is revised if there is a nonzero residual section force resultant, i.e., if ΣF_i-$N_{ext} \neq 0$; the algorithm converges to a final solution when both equilibrium requirements are satisfied.

The algorithm is summarized in the flowchart presented in Fig. 3. It comprises the following steps:

Step 1: For a selected level of sectional curvature, φ^n, it is required to calculate the associated moment resultant, M^n. (Note that problem unknowns are, the normal strain at the top fiber of the

jacketed cross section, $\varepsilon_{J1}^{n,m}$, the interface slip at the upper ($s_1^{n,r}$) and bottom interfaces ($s_2^{n,r}$) and the associated moment resultant, M^n). Therefore, start by setting the sectional curvature equal to φ^n

<u>*Step 2*</u>: Estimate normal strain at the top fiber of the cross section, $\varepsilon_{J1}^{n,m}$ [Fig. 1(a)]

<u>*Step 3*</u>: Estimate the interface slip at the upper and bottom interfaces, $s_1^{n,r}$ and $s_2^{n,r}$ [Eq. (16)]. Crack spacing is calculated from Eq. (11).

<u>*Step 4*</u>: Calculate the shear stress at the upper and bottom interfaces, $v_1^{n,r}$ and $v_2^{n,r}$, from the respective slip values, $s_1^{n,r}$ *and* $s_2^{n,r}$ [Eqs. (3-8)].

<u>*Step 5*</u>: Define shear stress demands, $v_{d,1}^{n,r}$ and $v_{d,2}^{n,r}$ [Eq. (12)]. If both $v_1^{n,r}= v_{d,1}^{n,r}$ and $v_2^{n,r}= v_{d,2}^{n,r}$ proceed to *Step 6*, otherwise return to *Step 3* and set $s_1^{n,r+1}=s_1^{n,r}+ds_1$, $s_2^{n,r+1}=s_2^{n,r}+ds_2$. ds_i is the selected increment in the slip value.

<u>*Step 6*</u>: Check cross section equilibrium. If $\Sigma F_i\text{-}N_{ext} \leq tolerance$ go to *Step 7*. In any other case return to *Step 2* and set $\varepsilon_{J1}^{n,m+1}=\varepsilon_{J1}^{n,m}+d\varepsilon_J$. $d\varepsilon_J$ is the step increment in the top strain of the jacketed cross section.

<u>*Step 7*</u>: Set $\varepsilon_{J1}^{n}=\varepsilon_{J1}^{n,m}$, $s_1^{n}=s_1^{n,r}$, $s_2^{n}=s_2^{n,r}$ and store convergent values.

<u>*Step 8*</u>: Estimate the moment resultant M^n. Repeat *Steps 1-7* for $n=n+1$. Calculations stop when the capacity of the shear interface is exhausted.

EXPERIMENTAL VALIDATION

Although RC jacketing is one of the most commonly applied rehabilitation methods worldwide, a limited number of experimental programs on RC jacketed subassemblages have been reported (Ersoy et al. 1993; Rodriguez and Park 1994; Bett et al. 1998; Gomes and Appleton 1998; Bousias et al. 2004; Vandoros and Dritsos 2006a, 2006b). The rather limited experimental database (compared to FRP jacketing, for example) is a serious impediment in the development of design expressions for this upgrading methodology.

In order to investigate the validity of the proposed analytical model for RC jacketed members published experimental data are used. From among the available tests those conducted by Rodriguez and Park (1994), Gomes and Appleton (1998), Bousias et al (2004) and Vandoros and Dritsos (2006a,

2006b) summarized in Table 1 are used for model verification as they are considered representative examples of columns under combined flexure and shear. It is noted that reinforcement slip owing to bond was included. Other relevant studies that were not included either concerned short column specimens (Bett et al. 1998), or tests that had been conducted under constant moment (no shear, Ersoy et al.1993).

Details of the experimental program are outlined in Table 1 for all specimens considered such as geometric properties and reinforcement details of the original as well as the jacketed elements. In the identification code adopted for the present comparative study the first character is either S or M corresponding to strengthened members with jacketing after cyclic loading or specimens built monolithically with a composite section to be used as controls, respectively. The second character represents the treatment at the interface: *r* corresponds to roughened interface achieved by chipping or sandblasting or other such methods, whereas *s* represents a smooth interface. The third character (D or N) identifies specimens with dowels (marked by D) or without dowels (marked by N) crossing the interface between the interior core and the jacket. The fourth character pd corresponds to pre-damaged units. The numerals 15, 25, 30 and 45 stand for the lap splice length of the existing unit corresponding to $15D_b$, $25D_b$, $30D_b$ and $45D_b$, respectively. The character *l* corresponds to U-shaped steel links utilized to connect the longitudinal reinforcement of the jacket to the existing member (core) and the character *w* corresponds to welding of stirrup ends of the first four stirrups (from the base of the jacketed member). The numeral in the end is the specimen number considered (in successive order) in Table 1. For easy reference, the original code names used for the specimens by the original investigators are also listed in Table 1 (column "Specimens").

Results

The calculated lateral load versus lateral displacement curves along with the curves obtained from standard sectional analysis of the monolithic cross sections for the total number of tested units are plotted in Figs. 4-8. The experimental curves plotted on the same Figure represent the envelope of the recorded lateral load versus lateral displacement hysteretic loops.

In general, the monolithic approach grossly overestimates the actual response of the jacketed

member; however it is successful in reproducing the *trends* of member behavior even if interface slip is neglected. The analytical model provides a lower bound of the response of the jacketed members and it may generally be considered conservative, while matching well the experimental values. At low deformation levels response curves obtained by the analytical approach and by the monolithic approach almost coincide. This is expected as long as crack formation is at an early stage.

In addition to these general observations, the following points are noted: for the first group of specimens (Rodriguez and Park 1994, Fig. 4) the previous damage of units S*r*Npd-1 and S*r*Npd-4 had no significant influence on the response as compared to units S*r*N-2 and S*r*N-3, which had not suffered any damage prior to jacketing. Clearly, the analytical result is very close to its experimental counterpart in the case of specimens M*s*N-7 and S*s*Npd-5 (Gomes and Appleton 1998, Fig. 5). The experimental curve representing specimen S*s*Npd-5 lies below that of specimen M*s*N-7 and this is attributed to the initial damage of unit S*s*Npd-5. In the third group (Bousias et al. 2004, Fig. 6) the experimental response of the units seems insensitive to the lap splice length of existing reinforcement and to the degree of previous damage imparted to units S*s*Npd15-12 and S*s*Npd25-13. This is also observed in the case of the fourth group of units (Bousias et al. 2004, Fig. 7). In the last group of units (Vandoros and Dritsos 2006a, 2006b, Fig. 8) the estimated strength of the monolithic unit (M*s*N-17) matches the experimental evidence but the actual secant to yield stiffness is lower. The response of unit S*s*N*w*-22 is very close to the response of the monolithic approach, although slip at the interface modifies the response somewhat, as shown by the analytical curve.

The response of the jacketed members is influenced greatly by the interface model utilized. A more sensitive model that could describe in more detail the interface shear behavior would provide better results. In general, a softer response than the experimental envelope implies too compliant an interface, whereas the opposite trend implies the interface stiffness has been overestimated. This is demonstrated in the following sections, where a parametric investigation of the model's sensitivity is explored. Interface behavior requires further calibration, and this would have been done if a critical mass of experiments were available. However, even as things stand, by explicitly accounting for this aspect in calculating the flexural response of composite members, the model introduces a degree of freedom that enables consideration of an important response mechanism that was previously

overlooked.

PARAMETRIC INVESTIGATION

A parametric investigation is conducted in the present section so as to establish the sensitivity of the monolithic factors to the important design and model variables. Note that these factors are used to estimate the response indices of jacketed, composite reinforced concrete members, from the corresponding response variables of monolithic members with identical cross section, on the premise that the latter quantities are easily established from conventional flexural analysis. The magnitude of monolithic factors depends on the property considered (strength, stiffness or deformation), on the jacket characteristics and on the interface properties.

Parameters of study

A sensitivity analysis of monolithic factors is conducted in this section through a detailed evaluation of two reference cases. The core of the composite member is the existing member, representative of former construction practices. In Case 1 the core used had a 350 mm square cross section, reinforced longitudinally with a steel area ratio, ρ_{lc}, equal to *1%* and transverse confining reinforcement ratio ρ_{wc}=0.13% (perimeter stirrups Ø6 mm/200 mm). Concrete cylinder uniaxial compressive strength $f_c^{/}$ was 16 MPa and steel yield strength f_{sy} was 300 MPa. In Case 2 the core had a rectangular cross section of 250 by 500 mm, with a longitudinal reinforcement ratio, ρ_{lc}=0.8%, transverse confining reinforcement ratio ρ_{wc}=0.24% (perimeter stirrups Ø8 mm/200 mm), concrete uniaxial compressive strength $f_c^{/}$=16 MPa and steel yield strength f_{sy}=300 MPa. In both cases the jacket considered was 75 mm thick. After application of the jacket the shear span ratio was reduced from 4.3 to 3 (flexure dominated) and from 3 to 2.3 (shear dominated) for the two case studies, respectively.

Parameters of the investigation were the percentage of the longitudinal reinforcement of the jacketed cross section ($\rho_{lJ}=A_J/(b_Jh_J-b_ch_c)$) which varied between 1% and 3%, the transverse confining reinforcement ratio of the jacket (ρ_{wJ}) which varied for the square cross section (Case 1) between 0.3% and 1.25% and for the rectangular cross section (Case 2) between 0.4% and 1.75% and the axial

load (N) applied on the jacketed cross section expressed as a fraction of the theoretical crushing capacity ($A_g f_c^{/}$) of the jacketed cross section which varied between 0 and 0.3. The cylinder compressive strength of the jacket concrete was taken as $f_c^{/}$=20 MPa. Yield strength of both longitudinal and transverse jacket reinforcements was taken as f_{sy}=500 MPa.

The results of the parametric study are presented in terms of the monolithic factor values both for flexural strength and for deformation capacities. In this regard, the following three definitions are adopted for the objectives of the study:

$$K_y^M = \frac{M_y}{M_{y,M}};\ K_u^M = \frac{M_u}{M_{u,M}} \tag{17.a}$$

$$K_y^\varphi = \frac{\varphi_y}{\varphi_{y,M}};\ K_u^\varphi = \frac{\varphi_u}{\varphi_{u,M}} \tag{17.b}$$

$$K^{\varphi,\mu} = \frac{\mu_\varphi}{\mu_{\varphi,M}};\ K^{\Delta,\mu} = \frac{\mu_\Delta}{\mu_{\Delta,M}} \tag{17.c}$$

where K^M, K^φ and K^μ refer to the monolithic factors for flexural strength, curvature and ductility. Subscripts y and u refer to yield and ultimate, respectively, whereas φ and Δ refer to curvature and displacement ductilities. The moments at yield, M_y, and ultimate, M_u, of the RC jacketed member are estimated by multiplying the corresponding moments, $M_{y,M}$, and $M_{u,M}$, of the monolithic member with factors K_y^M and K_u^M [Eq. (17.a)]. Pertinent monolithic factors K_y^φ and K_u^φ may be used in the same way in order to obtain the curvature at yield, φ_y, and ultimate, φ_u, of the RC jacketed members [Eq. (17.b)]. Similarly, by multiplying the curvature ductility $\mu_{\varphi,M}$ and the displacement ductility $\mu_{\Delta,M}$, of the monolithic cross section with appropriate monolithic factors $K^{\varphi,\mu}$ and $K^{\Delta,\mu}$, the curvature ductility μ_φ and the displacement ductility μ_Δ of the jacketed member may be estimated [Eq. (17.c)].

Role of the characteristics of the jacket

The direct effect induced by any change in the design characteristics of the jacket is depicted for both the yield and the ultimate stage in Fig. 9. The circular mark in Fig. 9 corresponds to the reference case of the parametric study with ρ_{lJ}= 1% ρ_{wJ}= 0.3% and $N^{/}$=0 for the square section example and ρ_{lJ}= 1% ρ_{wJ}= 0.4% and $N^{/}$=0 for the rectangular one. The arrows indicate the influence on the monolithic

factors plotted in the x and y axes, effected by a corresponding change in the parameter studied.

With reference to the square cross section (Case 1), increasing both the percentage of longitudinal reinforcement of the jacket (ρ_{lJ}) and the applied axial load ratio ($N'=N/A_g f_c'$) results in a reduction of K_y^M and an increase of K_y^φ [Fig. 9(a)]. This is also observed in the shear dominated member (Case 2), however, the influence is less pronounced especially on K_y^M. This indicates that flexure-dominated members are more sensitive to changes of axial load and longitudinal reinforcement compared to the shear-dominated ones. As discussed earlier, the jacketed member reaches yield at lower strength but at increased curvature as compared to its monolithic counterpart, owing to the increased deformation due to interface slip. The opposite is observed when confinement reinforcement of the jacket (ρ_{wJ}) is increased since interface slip is suppressed with confinement (i.e. the cross section approaches more the monolithic condition).

Results of the parametric investigation at a nominal ultimate limit state for both reference Cases 1 and 2 are presented in Fig. 9(b). The *nominal ultimate* is taken here to correspond to a lateral drift of 2% for both the analytical and monolithic model. This level was selected as a performance limit state and a point of reference as it corresponds to a displacement ductility in excess of 3 for regular frame members, which is considered an upper bound for the acceptable level of ductility demand in a redesigned structure. Increasing the longitudinal jacket reinforcement ratio (ρ_{lJ}) and applied axial load ratio (N') produce a simultaneous reduction in the monolithic factors for strength and deformation at ultimate, whereas the reverse effect is obtained by increasing the amount of jacket confinement reinforcement (ρ_{wJ}) [Fig. 9(b) for Case 1]. In the case of the shear-dominated member (Case 2) response is differentiated with regards to the axial load influence: as the axial load ratio increases the monolithic factor for strength at ultimate also increases, whereas the monolithic factor for deformation at ultimate decreases.

The influence that each of the parameters under investigation has on the various monolithic factors is depicted in Figs. 10, 11, 12 and is discussed in detail in the following paragraphs for both the square (Case 1) and rectangular (Case 2) cross sections, respectively.

Longitudinal jacket reinforcement ratio, (ρ_{lJ}): K_y^M, K_u^M, K_u^φ, $K^{\varphi,\mu}$, $K^{\Delta,\mu}$ are all reduced with increasing value of this variable [Fig. 10]. The reverse trend is observed for K_y^φ.

Axial load, (N'): Increasing the applied axial load ratio (N') leads to a simultaneous reduction of K_y^M, K_u^M and K_u^φ [Fig. 11], but also of $K^{\varphi,\mu}$ and $K^{\Delta,\mu}$. The monolithic factor of curvature at yield (K_y^φ) increases for an axial load ratio up to 0.2, but the trend is not uniform for both cases (Case 1 and 2) at higher axial loads.

Confining reinforcement, (ρ_{wJ}): As illustrated in Fig. 12, K_y^M and K_u^M increase mildly as the percentage of jacket confining reinforcement (ρ_{wJ}) increases. Because the dowel function of transverse reinforcement is mobilized passively, K_y^φ is almost insensitive to ρ_{wJ} whereas there is a strong increase of K_u^φ with confinement. Similarly, $K^{\varphi,\mu}$ and $K^{\Delta,\mu}$ both increase with ρ_{wJ}.

Discussion of the results of the parametric study

The results of the current parametric study provide an insight into the mechanical effect that jacket characteristics play on the lateral load response of jacketed members. Monolithic factors are sensitive to the design variables of the jacket and do not generally assume an obvious fixed value. From the results of the parametric study for both the square (Case 1) and the rectangular (Case 2) cross section the values of the monolithic factors range as follows (1) K_y^M=(0.63÷0.95), (2) K_u^M=(0.41÷0.97), (3) K_y^φ=(0.95÷3.12), (4) K_u^φ=(0.34÷0.90), (5) $K^{\varphi,\mu}$=(0.14÷0.93) and (6) $K^{\Delta,\mu}$=(0.37÷0.94).

The above results are consistent with the values suggested by EC8 [1996] for the monolithic factor of strength K_R=0.8 (no differentiation is made by the code between yield and ultimate), although the range of estimated values is larger for the ultimate (K_u^M). The estimated values for K_y^φ show that jacketed cross sections reach yield at greater curvatures, owing to slip at the interface between the existing member and the core. The K_u^φ is less than 1.0, thus, in general the curvature at ultimate (φ_u) estimated from the analytical approach is smaller than the monolithic estimate ($\varphi_{u,M}$). Considering that slip at the upper and bottom interfaces contributes to lateral drift, the reduced value of curvature at ultimate (2% drift) defined by the analytical approach is justified. The monolithic factors of curvature and displacement ductilities ($K^{\varphi,\mu}$, $K^{\Delta,\mu}$) are less than 1.0, which underlines that analytical curvature and displacement ductilities are both lower than the corresponding monolithic values.

SENSITIVITY OF THE ANALYTICAL MODEL

The proposed analytical model is primarily sensitive to parameters that affect the estimation of crack spacing and the shear strength of the contact interfaces. Each of these variables has a distinct influence on the computational procedure; however, selection of the shear interface model is fundamental. Variables of the shear transfer model used herein (Tassios and Vintzēleou 1987; Vintzēleou and Tassios 1986, 1987; Vassilopoulou and Tassios 2003) are the interface strength ($v_{c,u}$) and the slope of the postpeak branch (λ) [Fig. 13(a)].

A brief parametric investigation was conducted in order to explore the sensitivity of the model to the primary variables. The square cross section used in the preceding as Case 1 is used as a point of reference. Geometric characteristics and material properties of the existing member core were already given in earlier sections. Longitudinal jacket reinforcement ratio was selected as ρ_{lJ}=1%, with transverse confining reinforcement ρ_{wJ}=0.3% (f_{sy}=500 MPa). No axial load was applied on the jacketed cross section, whereas $f_c^{/}$=20 MPa for the jacket concrete.

First, the influence of the interface shear friction on the response of the jacketed member was studied. To model unfavorable conditions at the interface, the shear friction coefficient μ is increased stepwise up to 0.65 (values used are, 0.4, 0.55, 0.65 while keeping λ=1; this coefficient indirectly accounts for the roughness of the interface). The steepness of the descending branch was examined for λ=1, 1/2, and 1/3 whereas $v_{c,u}$ was given by Eq. (4). The values selected for λ are based on published experimental data (Bass et al. 1989; Papanicolaou and Triantafillou 2002). The results of the parametric investigation are summarized in Fig. 13 in a moment versus curvature diagram. For lower values of λ, i.e., more gradual decay of the descending branch of the shear stress strain curve [Fig.13(a)], higher levels of curvature capacity are estimated [Fig. 13(b)]. Increasing μ leads to higher shear capacity at the contact surface allowing for the development of higher strength and curvature values [Fig. 13(c)].

SUMMARY AND CONCLUSIONS

An algorithm for calculating the monotonic response of reinforced concrete jacketed members is presented. The model introduces a kinematic degree of freedom (interface slip) that enables consideration of an important mechanism of behavior that was previously overlooked, namely the shear transfer mechanisms mobilized due to sliding at the interface between existing and new material. The weak link controlling deformations in this problem is the interface. The capacity of the weakest link is evaluated and checked in every step, to make sure it is not exceeded by the demand. The shear demand at the interface is controlled by the flexural stresses on the cross section and by the spacing of cracks in the longitudinal direction, whereas the shear capacity is a function of slip. The shear stress slip relationship for the contact surfaces and the definition of crack spacing play a key role in the algorithm. Analytical results show that the model can reproduce successfully the observed response of jacketed members and correlates well with experimental data. This analysis tool was used to explore the difference between the ideal response of monolithic members and the actual response of the RC jacketed members of identical geometry with reference to the design variables. A parametric study was conducted and the dependence of various monolithic factors on the characteristics of the jacket was investigated. It was found that strength factors at yield (K_y^M) range between 0.63 and 0.95, whereas strength factors at ultimate (K_u^M) range between 0.41 and 0.97. Monolithic factors for deformation indices were found in case of curvature at yield to range between 0.95 and 3.12, whereas in case of curvature at ultimate between 0.34 and 0.90. The monolithic factors of curvature and displacement ductilities ($K^{\varphi,\mu}$, $K^{\Delta,\mu}$) are both lower than the corresponding monolithic values with the former to range between 0.14 and 0.93 and the latter between 0.37 and 0.94.

ACKNOWLEDGMENTS

The first author was co-funded by the European Research Project "Seismic Performance Assessment and Rehabilitation" (SPEAR), through Imperial College of Science, Technology and Medicine (London, UK) and by the Hellenic Ministry of Education and Religion Affairs through the scholarship "HRAKLEITOS". The contribution of the second author was funded by the Hellenic Secretariat of

Research and Technology (GSRT) through the multi-Institutional Project "ARISTION". The contribution of the third author was funded by the US National Science Foundation through the Mid-America Earthquake Center, Award Number EEC 97-01785.

NOTATION

The following symbols are used in this paper:

A_g = gross section area;

A_{int} = contact area of the interface;

D_b = diameter of the bars clamping the interface;

$D_{b,c}$, D_{bJ} = bar diameter of the core and the jacket longitudinal reinforcement, respectively;

E_s = elastic modulus of steel;

E_{cm} = elastic modulus of concrete;

I = moment of inertia of the composite cross section;

K_i = monolithic factor, where the subscript i=R, K refers to strength and stiffness, respectively;

K^M, K^φ, K^μ = monolithic factors for flexural strength, curvature and ductility, respectively;

L_s = shear span of the member;

M = moment resultant;

N = axial load;

N' (=$N/A_g f_c'$)= applied axial load ratio;

N_c , N_J = number of bars in the tension steel layer of the core and the jacket, respectively;

N_{ext} = externally applied axial load;

S_i = first moment of area;

V = shear force on the member;

$V_D(s)$ = dowel force estimated for slip magnitude, s;

$V_{D,u}$ = ultimate dowel force;

b_J = width of the jacketed cross section;

c = average crack spacing;

$f_{b,c}$, $f_{b,J}$ = average bond stress of the core and the jacket reinforcement layer, respectively;

$f_c^{/}$ = concrete cylinder uniaxial compressive strength;

f_{ctm} = tensile strength of concrete;

$f_{ctm,c}$ = tensile strength of concrete core;

f_s = axial stress of the bars crossing the interface;

$f_{s,cr}$ = jacket steel stress at the crack;

f_{sy} = yield strength of steel;

j_d = distance between the upper and the bottom interfaces;

k = number of dowels;

l_c = height of the tension zone in the core component of the composite cross section;

l_p = length of the plastic hinge region;

p = normal pressure externally applied on the contact plane;

q_s = shear flow at the contact between the bottom layer and the core;

q_o = shear flow based on classical mechanics;

s = lateral slip;

s_{1u}, s_{2u} = slip values at the upper and bottom interfaces of the jacket;

$s_{c,u}$ = ultimate slip value beyond which the frictional mechanisms breakdown;

$s_{d,el}$ = elastic slip value;

$s_{d,u}$ = ultimate slip value;

v_1 , v_2 = shear resistances at the upper and bottom interfaces;

v_a = shear resistance of the aggregate interlock mechanism;

$v_c(s)$ = frictional resistance at slip, s;

$v_{c,u}$ = ultimate frictional resistance of the interface;

v_D = shear stress resisted by dowel action in cracked reinforced concrete;

$v_{d,1}$, $v_{d,2}$ = shear demand values;

v_n = shear resistance;

w = separation between contact surfaces as they slide overriding one another;

<u>*Greek symbols*</u>:

$\Delta\varepsilon_1$, $\Delta\varepsilon_2$ = magnitude of strain discontinuity at the upper and bottom interfaces, respectively;

$\Delta_{p,u}$ = plastic displacement;

$\Delta_{slip,u}$ = displacement owing to interface slip;

Δ_y = elastic displacement at yield;

Δ_o = total tip displacement;

ΣF_i = normal stress resultant of each layer, i;

α = bar axial stress normalized with respect to its yield value;

ε_{c1}, ε_{j2}, ε_{j3}, ε_{c2} = normal strains in the section layers above and below the contact surfaces;

ε_c = concrete strain at the extreme compression fiber;

ε_{sy} = tensile reinforcement yield strain;

$\eta(=E_s/E_{cm})$ = modular ratio;

$\theta_{slip,u}$ = rotation owing to interface slip;

λ = coefficient indirectly accounting for the roughness of the interface;

μ = interface shear friction coefficient;

μ_Δ = displacement ductility;

μ_φ = curvature ductility;

ρ_{lc} = percentage of the longitudinal reinforcement of the existing cross section (core);

ρ_{lJ} = percentage of the longitudinal reinforcement of the jacketed cross section;

ρ_s = reinforcement area ratio

$\rho_{s,eff}$ = effective reinforcement ratio;

ρ_{wc} = transverse confining reinforcement ratio of the existing cross section (core);

ρ_{wJ} = transverse confining reinforcement ratio of the jacketed cross section;

σ_N = normal clamping stress acting on the interface;

τ_{xy} = shear stress acting on a plane with unit normal parallel to x axis, and oriented in the y axis (defined according to classical mechanics as per Fig. 2)

τ_{xz} = shear stress acting on a plane with unit normal parallel to x axis, and oriented in the z axis, respectively [Fig. 1(d)].

φ = curvature;

φ_y = curvature at yield of the composite section;

$\varphi_{y,M}$ = curvature at yield of the monolithic cross section;

φ_u = curvature at ultimate; and

$\varphi_{u,M}^{eq}$ = equivalent monolithic curvature.

REFERENCES

Bass, R. A., Carasquillo, R. L., and Jirsa, J. O. (1989). "Shear transfer across new and existing reinforced concrete." *ACI Struct. J.*, 86(4), 383-393.

Bett, B. J., Klinger, R. E., and Jirsa, J. O. (1998). "Lateral load response of strengthened and repaired r.c. columns." *ACI Struct. J.*, 85(5), 499-507.

Bousias, S., Spathis, A., and Fardis M. (2004). "Seismic retrofitting of columns with lap-splices via RC jackets." *Proc., 13th World Conf. Earthq. Eng.*, Canadian Association of Earthquake Engineering (CAEE), Vancouver, B.C., Canada, Paper No. 1937.

CEB-FIP Model Code 90 (1993). "Design Code." Thomas Telford Ltd., eds., London, 460.

Ersoy, U., Tankut, T., and Suleiman, R. (1993). "Behavior of jacketed columns." *ACI Struct. J.*, 93(3), 288-293.

Eurocode 8 (1996). "Design provisions for earthquake resistance of structures. Part 1.4: General rules - Strengthening and repair of buildings (Annex G)."ENV 1998-1-4, European Committee for Standardization (CEN), Brussels.

fib Bulletin 24 (2003). "Seismic assessment and retrofit of reinforced concrete buildings." *federation international du béton (fib),* State-of-the-art report, 312.

Gomes, A. M., and Appleton J. (1998). "Repair and strengthening of R.C. elements under cyclic loading." *Proc., 11th Europ. Conf. Earthq. Eng.*, A.A. Balkema (Rotterdam, The Netherlands), Paris, France, CD-ROM.

KANEPE (2004). "Requirements for Seismic Rehabilitation of Buildings." *Earthquake Planning and Protection Organization (E.P.P.O.),* First Draft – February 2004 (in Greek).

Papanicolaou, C., and Triantafillou, T. (2002). "Shear transfer capacity along pumice aggregate

concrete and hpc interfaces." *Mat. and Structures J.*, 35(248), 237-245.

Paulay, T., and Priestley, M. J. N. (1992). "Seismic design of reinforced concrete and masonry buildings." Wiley, eds., New York, 744.

Rodriguez, M., and Park, R. (1994). "Seismic load tests on reinforced concrete columns strengthened by jacketing." *ACI Struct. J.*, 91(2), 150-159.

Tassios, T., and Vintzēleou, E. (1987). "Concrete-to-concrete friction." *ASCE J. Struct. Eng.*, 113(4), 832-849.

Vandoros, K. G. and Dritsos, S. E. (2006a). "Interface treatment in shotcrete jacketing of reinforced concrete columns to improve seismic performance." *J. Struct. Eng. and Mech.*, 23(1), 43-61.

Vandoros, K. G. and Dritsos, S. E. (2006b). "Axial preloading effects when reinforced concrete columns are strengthened by concrete." *Progress in Struct. Eng. and Mat. J.*, 8(3), 79-92.

Vassilopoulou, I., and Tassios, P. (2003). "Shear transfer capacity along a r.c. crack under cyclic sliding." *Proc., fib Symposium*, TCG (Technical Chamber of Greece), Athens, Greece, Paper No. 271.

Vecchio, F. J., and Collins, M..P. (1988). "Predicting the response of r.c. beams subjected to shear using the MCFT." *ACI Journal*, 86(3), 258-268.

Vintzēleou, E., and Tassios, T. (1986). "Mathematical models for dowel action under monotonic and cyclic conditions." *Magaz. of Concrete Research*, 38(134), 13-22.

Vintzēleou, E., and Tassios, T. (1987). "Behavior of dowels under cyclic deformations." *ACI Struct. J.*, 84(1), 18-30.

List of Captions

Tables:

Table 1. Summary of test unit properties.

Figures:

Fig. 1. (a) Strain profiles; (b) Normal stresses at the interface; (c) pull-out displacement of the bars crossing the interface; (d) state of stress acting on an infinitesimal element in the initial coordinate system.

Fig. 2. (a), (b) Definition of crack spacing; (c) Estimation of vertical shear stress τ_{xy}, denoted here as v_{di}; (d) Rotation of the jacketed cross section due to slip.

Fig. 3. Flowchart of the proposed algorithm.

Fig. 4. Lateral load versus drift for the 1st Group of units (Rodriguez and Park 1994).

Fig. 5. Lateral load versus drift for the 2nd Group of units (Gomes and Appleton 1998).

Fig. 6. Lateral load versus drift for the 3rd Group of units (Bousias et al. 2004).

Fig. 7. Lateral load versus drift for the 4th Group of units (Bousias et al. 2004).

Fig. 8. Lateral load versus drift for the 5th Group of units (Vandoros and Dritsos 2006a, 2006b).

Fig. 9. Monolithic factors of strength and deformation at (a) yield and (b) ultimate.

Fig. 10. Influence of jacket longitudinal reinforcement on monolithic factors (*Case 1*, *Case 2*).

Fig. 11. Influence of axial load on monolithic factors (*Case 1*, *Case 2*).

Fig. 12. Influence of jacket confinement reinforcement on monolithic factors (*Case 1*, *Case2*).

Fig. 13. Role of the shear friction interface model.

Table 1. Summary of test units

Group	Code Name[≋]	Specimen[‡]	b_c^*	h_c^*	$D_{b,c}^*$	$\rho_{lc}^{\#}$	$D_{bs,c}^*$	$p_{wc}^{\#}$	$f_c'^{\S}$	$f_{sy}^{\S}$	b_J^*	h_J^*	$D_{b,J}^*$	$\rho_{lJ}^{\#}$	$D_{bs,J}^*$	$\rho_{wJ}^{\#}$	$f_c'^{\S}$	$f_{sy}^{\S}$	N'^*	L_s^*
1st Rodriquez & Park (1994)	S*r*Npd-1	SS1	350	350	20	2.05	6	0.16	29.5	325	550	550	16	0.89	10	0.36	32.9	502	10.0	1425
	S*r*N-2	SS2	350	350	20	2.05	6	0.16	29.5	325	550	550	16	0.89	10	0.36	34.0	502	10.0	1425
	S*r*N-3	SS3	350	350	20	2.05	6	0.16	29.5	325	550	550	12	0.75	10	0.94	19.4	491	10.0	1425
	S*r*Npd-4	SS4	350	350	20	2.05	6	0.16	25.9	325	550	550	12	0.75	10	0.94	25.2	491	10.0	1425
2nd Gomes & Appleton (1998)	S*s*Npd-5	P2R	200	200	12	1.13	6	0.22	53.2	480	260	260	12	1.64	6	0.33	58.2	480	6.0	1000
	S*s*Npd-6	P3R	200	200	12	1.13	6	0.66	58.2	480	260	260	12	1.64	6	0.49	49.6	480	7.1	1000
	M*s*N-7	P4	200	200	12	1.13	6	0.22	56.2	480	260	260	12	1.64	6	0.33	56.2	480	6.3	1000
3rd Bousias et al. (2004)	M*s*N-8	Q-RCL0M	250	250	14	0.98	8	0.24	30.6	313	400	400	20	1.29	10	0.44	30.6	500	18.0	1600
	S*s*N-9	Q-RCL0	250	250	14	0.98	8	0.24	26.3	313	400	400	20	1.29	10	0.44	55.8	500	7.9	1600
	S*s*N15-10	Q-RCL1	250	250	14	0.98	8	0.24	27.5	313	400	400	20	1.29	10	0.44	55.8	500	8.4	1600
	S*s*N25-11	Q-RCL2	250	250	14	0.98	8	0.24	25.6	313	400	400	20	1.29	10	0.44	55.8	500	8.4	1600
	S*s*Npd15-12	Q-RCL01pd	250	250	14	0.98	8	0.24	28.1	313	400	400	20	1.29	10	0.44	20.7	500	25.0	1600
	S*s*Npd25-13	Q-RCL02pd	250	250	14	0.98	8	0.24	28.6	313	400	400	20	1.29	10	0.44	20.7	500	27.0	1600
4th Bousias et al. (2004)	S*s*N15-14	R-RCL1	250	500	18	0.81	8	0.24	36.7	514	400	650	18	1.13	10	0.44	55.8	500	6.6	1600
	S*s*N30-15	R-RCL3	250	500	18	0.81	8	0.24	36.8	514	400	650	18	1.13	10	0.44	55.8	500	6.6	1600
	S*s*N45-16	R-RCL4	250	500	18	0.81	8	0.24	36.3	514	400	650	18	1.13	10	0.44	55.8	500	5.2	1600
5th Vandoros and Dritsos (2006a, 2006b)	M*s*N-17	Q-RCM	250	250	14	0.98	8	0.24	24.7	313	400	400	20	1.29	10	0.44	24.7	487	21.2	1600
	S*s*N*l*-18	Q-RCW	250	250	14	0.98	8	0.24	22.9	313	400	400	20	1.29	10	0.44	18.8	487	21.6	1600
	S*s*D-19	Q-RCD	250	250	14	0.98	8	0.24	27.0	313	400	400	20	1.29	10	0.44	55.8	487	8.9	1600
	S*r*N-20	Q-RCR	250	250	14	0.98	8	0.24	27.0	313	400	400	20	1.29	10	0.44	55.8	487	8.9	1600
	S*r*D-21	Q-RCRD	250	250	14	0.98	8	0.24	27.0	313	400	400	20	1.29	10	0.44	55.8	487	8.9	1600
	S*s*N*w*-22	Q-RCNT	250	250	14	0.98	8	0.24	27.0	313	400	400	20	1.29	10	0.44	17.8	487	25.6	1600
	S*s*N-23[†]	Q-RCNTA	250	250	14	0.98	8	0.24	23.8	313	400	400	20	1.29	10	0.44	34.5	487	11.8	1600
	S*s*D*w*-24	Q-RCE	250	250	14	0.98	8	0.24	36.8	313	400	400	20	1.29	10	0.44	24.0	487	20.6	1600

[≋]S: strengthened members with jacketing, M: specimens built monolithically, *r*: roughened interface, *s*: smooth interface, D, N: specimens with or without dowels, respectively, *pd*: pre-damaged units, 15, 25, 30 and 45: stand for the lap splice length corresponding to $15D_b$, $25D_b$, $30D_b$ and $45D_b$, *l*: U-shaped steel links utilized, *w*: welding of stirrup ends of the first four stirrups, the numeral in the end is the specimen number considered (in successive order), [‡] original code names used for the specimens by the original investigators [*]mm, [#] %, [§] MPa, [*]axial load ratio % calculated on the basis of concrete strength of the jacket, [†]Jacket constructed under axial load

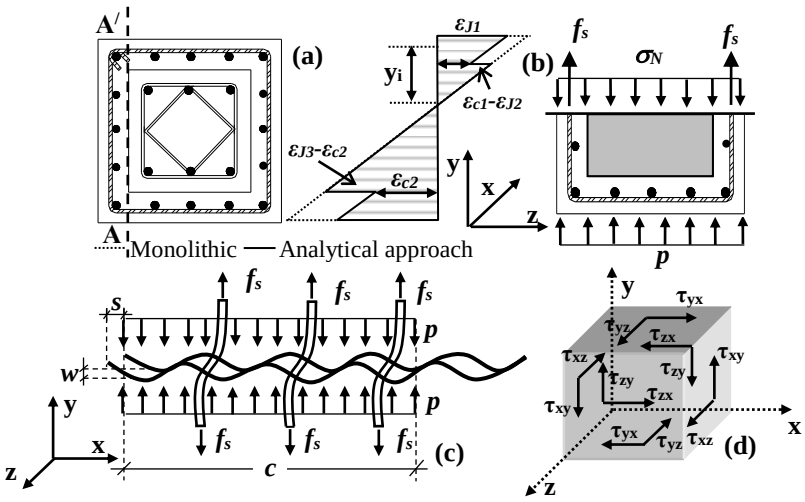

Fig. 1. (a) Strain profiles; (b) Normal stresses at the interface; (c) pull-out displacement of the bars crossing the interface; (d) state of stress acting on an infinitesimal element in the initial coordinate system.

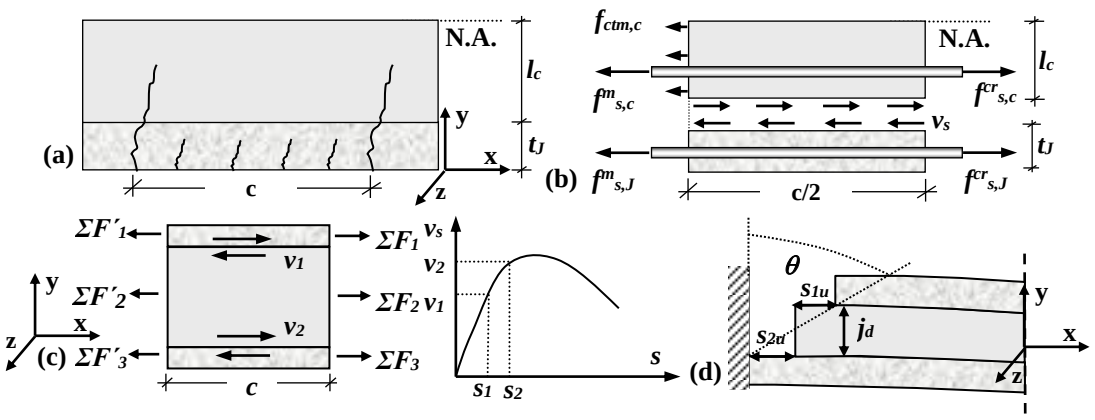

Fig. 2. (a), (b) Definition of crack spacing; (c) Estimation of vertical shear stress τ_{xy}, denoted here as v_{di}; (d) Rotation of the jacketed cross section due to slip.

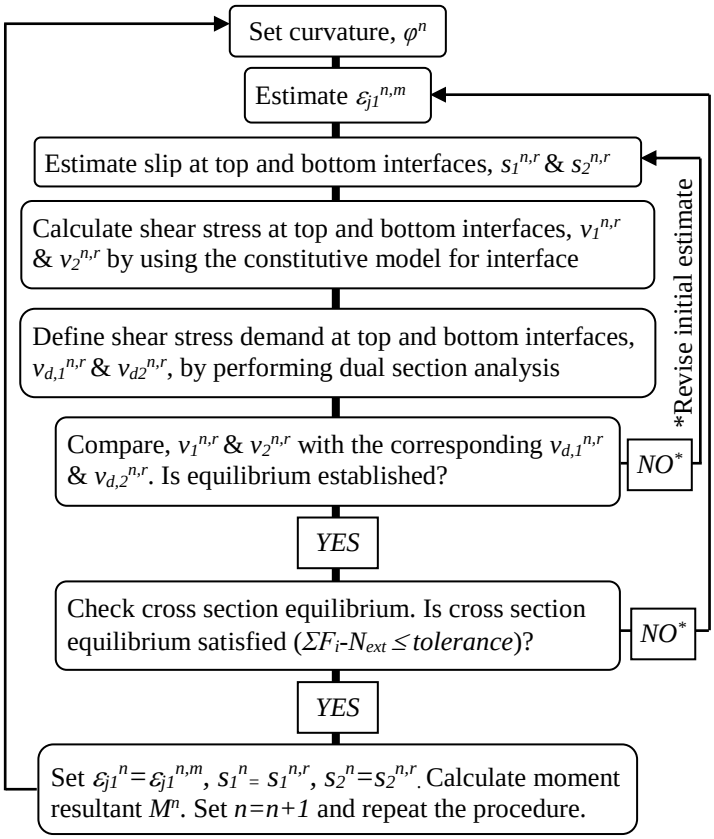

Fig. 3. Flowchart of the proposed algorithm.

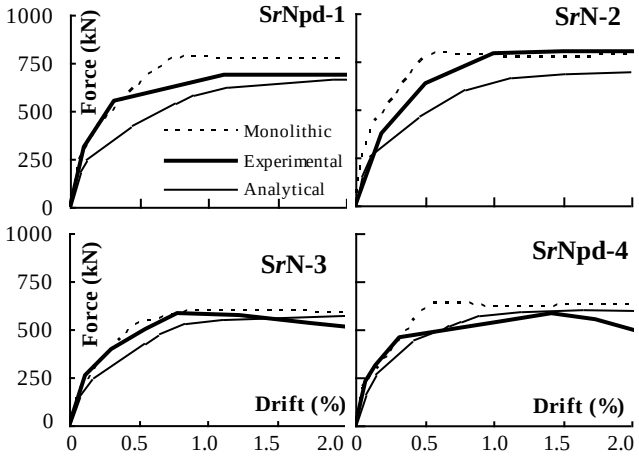

Fig. 4. Lateral load versus lateral drift for the 1st Group of units (Rodriguez and Park 1994).

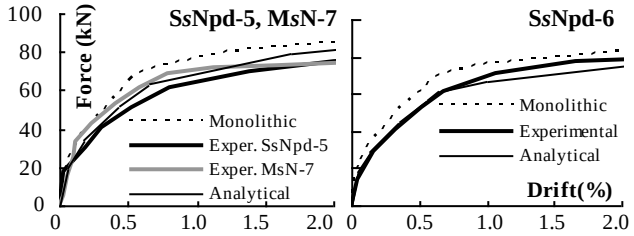

Fig. 5. Lateral load versus lateral drift for the 2nd Group of units (Gomes and Appleton 1998).

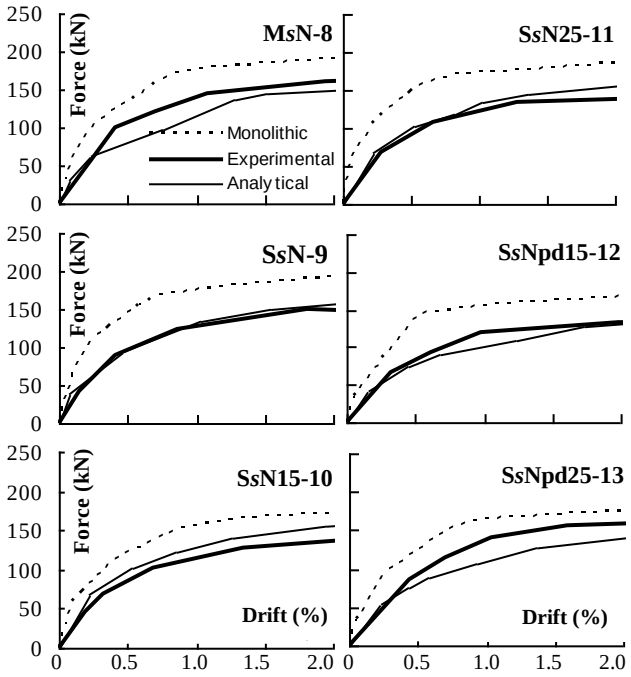

Fig. 6. Lateral load versus lateral drift for the 3rd Group of units (Bousias et al. 2004).

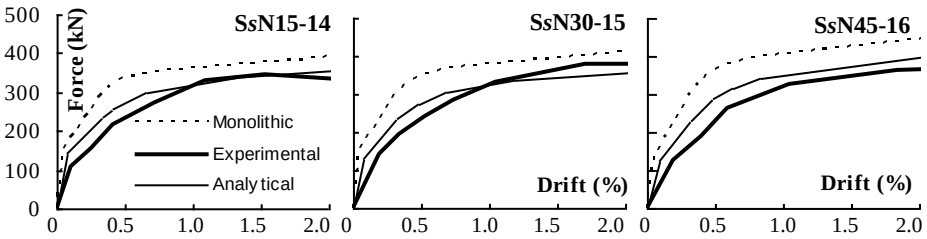

Fig. 7. Lateral load versus lateral drift for the 4th Group of units (Bousias et al. 2004).

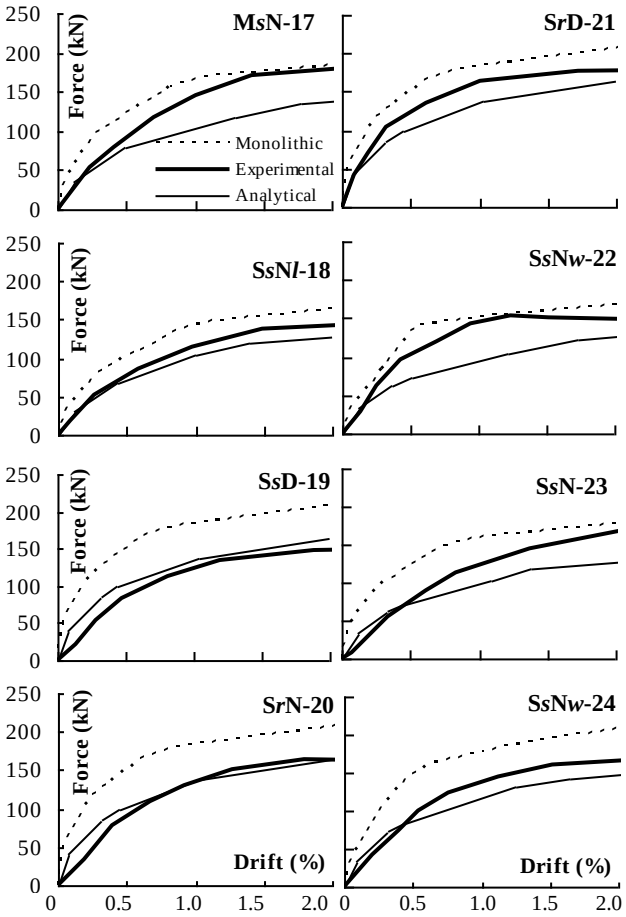

Fig. 8. Lateral load versus lateral drift for the 5th Group of units (Vandoros and Dritsos 2006a, 2006b).

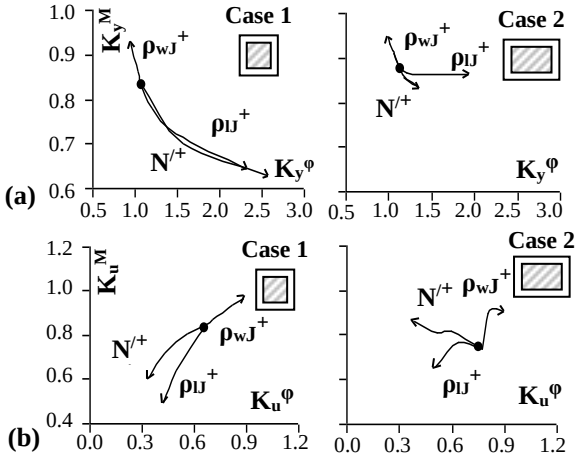

Fig. 9. Monolithic factors of strength and deformation at (a) yield and (b) ultimate.

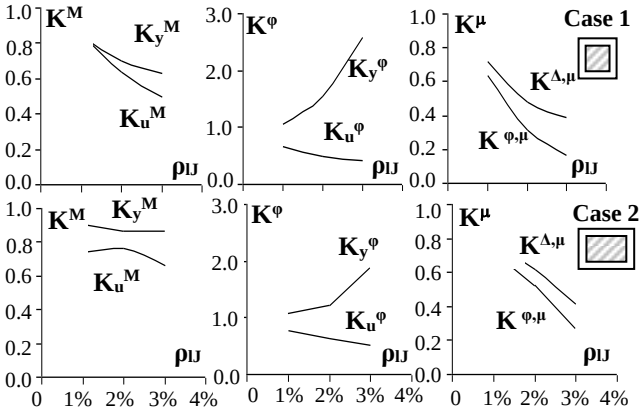

Fig. 10. Influence of jacket longitudinal reinforcement on monolithic factors (*Case 1*, *Case 2*).

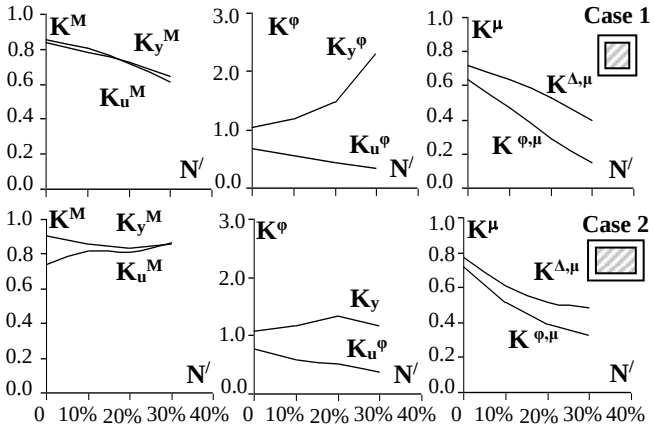

Fig. 11. Influence of axial load on monolithic factors (*Case 1*, *Case 2*).

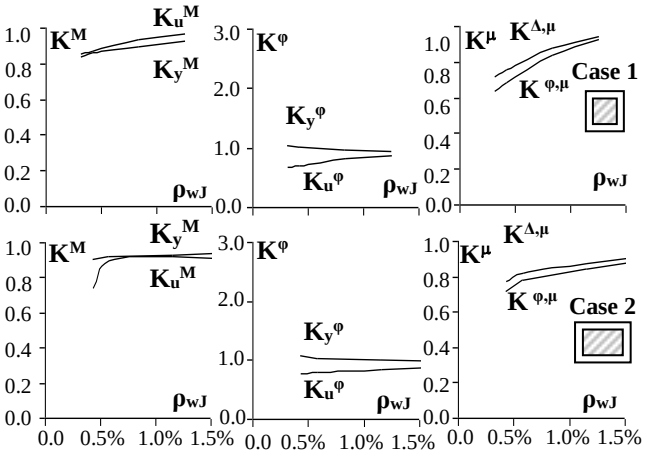

Fig. 12. Influence of jacket confinement reinforcement on monolithic factors (*Case 1*, *Case2*).

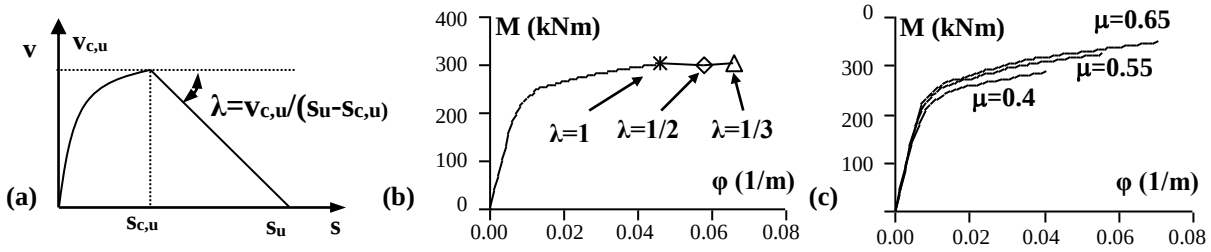

Fig. 13. Role of the shear friction interface model.